Journal of Alloys and Compounds 611 (2014) 292–296

Contents lists available at ScienceDirect

Journal of Alloys and Compounds

journal homepage: www.elsevier.com/locate/jalcom

Crystalline to amorphous transition in solids upon high-pressure torsion

R.V. Sundeev [a,b,*], A.M. Glezer [a,b,c], A.V. Shalimova [a]

[a] I.P. Bardin Central Research Institute for Ferrous Metallurgy, 2-ya Baumanskaya 9/23, Moscow 105005, Russia
[b] Moscow State University of Instrument Engineering and Computer Science, Stromynka 20, Moscow 107996, Russia
[c] National University of Science and Technology "MISIS", Leninsky avenue 4, Moscow 119049, Russia

ARTICLE INFO

Article history:
Received 29 March 2014
Received in revised form 14 May 2014
Accepted 15 May 2014
Available online 24 May 2014

Keywords:
Amorphous materials
Thermodynamic properties
Phase transformation
Amorphization

ABSTRACT

The amorphization behavior of the crystalline multicomponent $Ni_{50}Ti_{30}Hf_{20}$, $Ti_{50}Ni_{25}Cu_{25}$, $Zr_{50}Ni_{18}Ti_{17}Cu_{15}$, and $Fe_{78}B_{8.5}Si_9P_{4.5}$ alloys upon severe plastic deformation (SPD) has been studied. It is shown that the crystalline to amorphous transition is determined by the ability of the crystals to accumulation of deformation defects under mechanical action, by the thermodynamic stability of the crystalline phases contained in the alloy, and by the possibility of the diffusion processes necessary for the change in the chemical composition of the crystalline and amorphous phases upon deformation. It is found that the susceptibility to amorphization upon SPD does not coincide with the tendency of the alloys to amorphization upon melt quenching.

1. Introduction

The method of melt quenching is most effective for the realization of an amorphous state in metal alloys [1]. However in recent years the severe plastic deformation (SPD) of crystalline metallic materials has been used for production of amorphous state [2,3]. Furthermore simultaneously two amorphous phases with different composition has been detected in $Ni_{50}Nb_{20}Y_{30}$ crystalline alloy driven by SPD [4]. Highly profitable method of attack for prediction of possible phase initiation including amorphous one under SPD has been proposed in studies [5,6]. The basis for it is the introduction of the effective temperature as a parameter of SPD by analogy with irradiation process [7]. This parameter allows to estimate the character of phase transformations in accordance to phase diagram for given alloy composition. We reason however that structural evolution driven by SPD differ noticeably from the another modes of external effects. Therefore, the physical parameters which control the ability of crystals to amorphization by SPD are not yet estimated to completion.

The aim of this work is to identify the main factors determining the transition of crystalline alloys to the amorphous state upon high-pressure torsion (HPT) and to compare this effect for the alloys characterized by the ability to thermal amorphization (ATA) upon melt quenching.

2. Experimental

The crystalline samples for deformation were obtained by annealing of the amorphous $Ni_{50}Ti_{30}Hf_{20}$, $Ti_{50}Ni_{25}Cu_{25}$, $Zr_{50}Ni_{18}Ti_{17}Cu_{15}$, and $Fe_{78}B_{8.5}Si_9P_{4.5}$ metal alloys prepared from pure components by melt quenching in argon. The $Ni_{50}Ti_{30}Hf_{20}$, $Ti_{50}Ni_{25}Cu_{25}$, and $Zr_{50}Ni_{18}Ti_{17}Cu_{15}$ amorphous alloys were annealed in air at 500–510 °C for 30 min, and the $Fe_{78}B_{8.5}Si_9P_{4.5}$ alloy was annealed by two regimes, at 540 °C for 30 s and at 600 °C for 25 min. The latter treatment allowed us to obtain virtually single-phase (1) and two-phase (2) states for the iron-based alloy. All samples were deformed by high-pressure torsion at a hydrostatic pressure of 4 GPa at room temperature. The rotation rate of the movable anvil was about 1 rpm. The total number of revolutions $\boldsymbol{n}$ of the mobile anvil was varied from 1/4 to 9. The structure and phase composition were examined by the methods of transmission electron microscopy (TEM) and X-ray diffraction (XRD). The volume fraction of the amorphous phase was calculated by the XRD data.

3. Result and discussion

The full X-ray patterns corresponding to all of the studied alloys are presented in Fig. 1. A comparison of the X-ray patterns obtained for the deformed samples allows us to conclude that the spectrum profile changes from the crystalline to the X-ray amorphous state with the accumulation of deformation (an increase in the revolution number $\boldsymbol{n}$ of the rotating anvil). The change in the crystalline phase fraction $\boldsymbol{V}$ in the alloys with increasing degree of deformation was defined, and the $\boldsymbol{V}^*(\boldsymbol{n})$ dependence was constructed (Fig. 2). The volume fraction in Fig. 2 was normalized to 100% of the initial crystalline phase at $\boldsymbol{n} = 0$ ($\boldsymbol{V}^*$), since a small amount (~10 vol.%) of the amorphous phase was retained in each alloy in the initial crystalline state for the facilitation of deformation.

* Corresponding author at: I.P. Bardin Central Research Institute for Ferrous Metallurgy, 2-ya Baumanskaya 9/23, Moscow 105005, Russia. Tel.: +7 9168279693.
E-mail address: apricisvir@gmail.com (R.V. Sundeev).

http://dx.doi.org/10.1016/j.jallcom.2014.05.109
0925-8388/

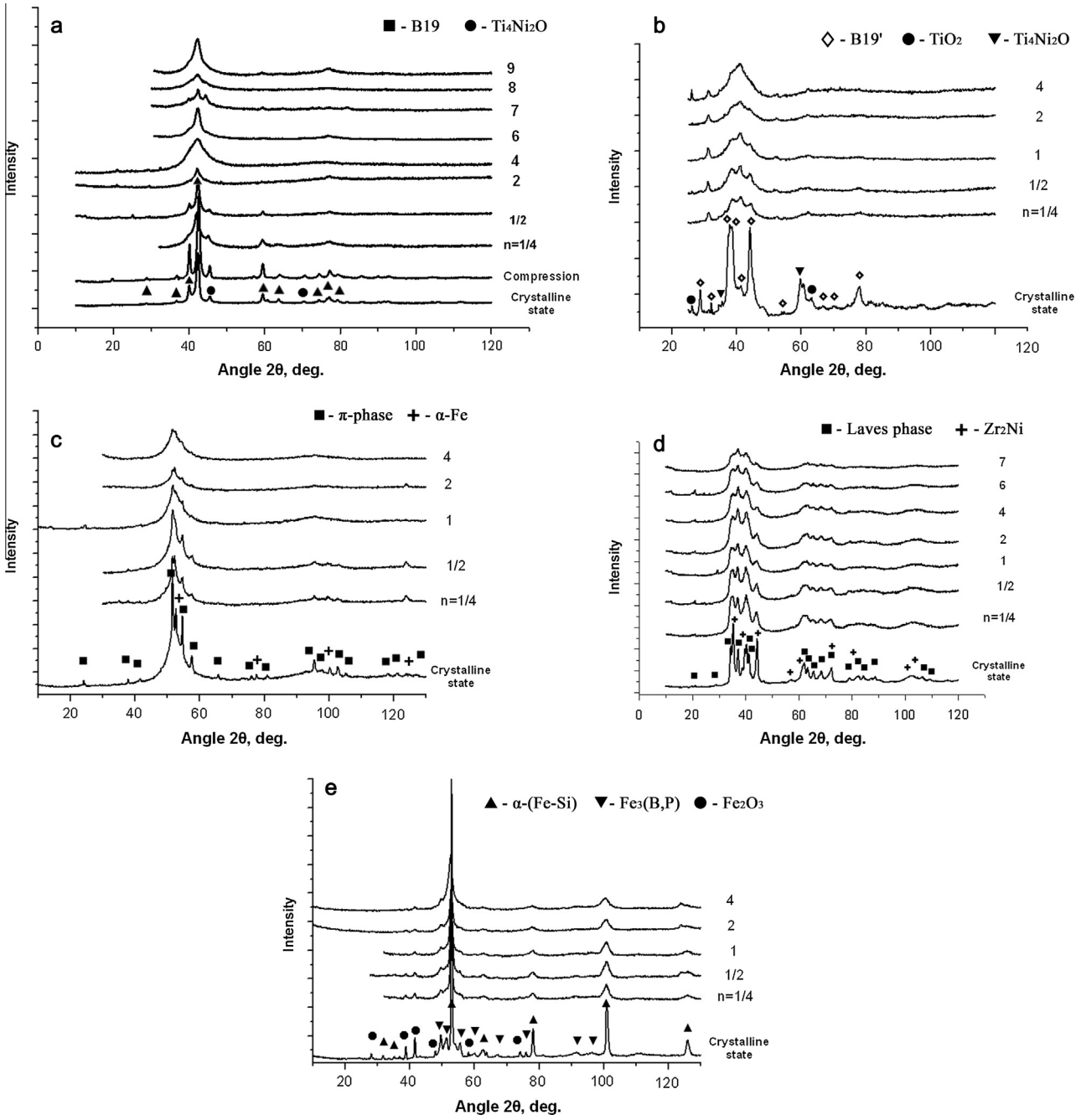

Fig. 1. X-ray diffraction patterns for alloys: (a) $Ti_{50}Ni_{25}Cu_{25}$, (b) $Ni_{50}Ti_{30}Hf_{20}$, (c) $Fe_{78}B_{8.5}Si_9P_{4.5}$ (1), (d) $Zr_{50}Ni_{18}Ti_{17}Cu_{15}$ and (e) $Fe_{78}B_{8.5}Si_9P_{4.5}$ (2) after HPT.

The slope of the $\boldsymbol{V}^*(\boldsymbol{n})$ dependence characterizes the ability to deformation-induced amorphization (ADIA) $\boldsymbol{\kappa_a} = |\boldsymbol{dV}^*/\boldsymbol{dn}|$. The $\boldsymbol{\kappa_a}$ values of the alloys are given in Table 1.

As is seen from Table 1 and Fig. 2, the alloys can be divided into two groups:

- Alloys with high ADIA $\boldsymbol{\kappa_a}$ (the first group), the $Ni_{50}Ti_{30}Hf_{20}$, $Ti_{50}Ni_{25}Cu_{25}$, and $Fe_{78}B_{8.5}Si_9P_{4.5}$ alloys (1) in the single-phase state.
- Alloys with low ADIA $\boldsymbol{\kappa_a}$ (the second group), the $Zr_{50}Ni_{18}Ti_{17}Cu_{15}$ and $Fe_{78}B_{8.5}Si_9P_{4.5}$ alloys (2) in the two-phase state.

The $Ni_{50}Ti_{30}Hf_{20}$ and $Ti_{50}Ni_{25}Cu_{25}$ alloys of the first group after annealing are in the B19 or B19′ single-phase state with a characteristic plate martensite structure (Fig. 3a). After deformation to $\boldsymbol{n} = 2$, the X-ray amorphous state of the $Ni_{50}Ti_{30}Hf_{20}$ and $Ti_{50}Ni_{25}Cu_{25}$ alloys is achieved [8].

The examination of the structure and phase composition of the $Fe_{78}B_{8.5}Si_9P_{4.5}$ alloy (1) showed that annealing at 540 °C for 30 s leads to the formation of the metastable tetragonal π phase (which is the structural analog of β-Mn, $a = 0.619$ nm) [9] with an average particle size of about 100 nm (Fig. 4a). In this structural state, the $Fe_{78}B_{8.5}Si_9P_{4.5}$ alloy (1) undergoes the amorphization relatively quickly (for $\boldsymbol{n} = 4$).

In the second-group $Zr_{50}Ni_{18}Ti_{17}Cu_{15}$ alloy, the phase composition is a mixture of two crystalline phases in an approximate ratio of 1:1. These phases are Zr_2Ni (the $CuAl_2$ structure type) and the Zr–Ti (Ni, Cu) Laves phase (the $MgZn_2$ structure type) (Fig. 5a) [10].